Nonreciprocal Thermal Emitters Using Metasurfaces with Multiple Diffraction Channels

Bo Zhao,[1,†] Jiahui Wang,[2] Zhexin Zhao,[1] Cheng Guo,[2] Zongfu Yu,[3] and Shanhui Fan[1,*]

[1] *Department of Electrical Engineering, Stanford University, Stanford, California 94305, USA*

[2] *Department of Applied Physics, Stanford University, Stanford, California 94305, USA*

[3] *Department of Electrical and Computer Engineering, University of Wisconsin, Madison, Wisconsin 53706, USA*

(Received 11 August 2021; revised 11 October 2021; accepted 5 November 2021; published 1 December 2021)

The emissivity and absorptivity of nonreciprocal thermal emitters are not constrained by the well-known Kirchhoff law of thermal radiation, which usually serves as the theoretical basis to characterize thermal properties. When thermal emitters are nondiffracting, which is the case in previous studies of nonreciprocal thermal emitters, the angular distribution of emissivity and absorptivity is mirror symmetric with respect to the normal direction, and the nonreciprocal effect is confined to a relatively narrow angular range. In this work, we consider nonreciprocal thermal emitters that can simultaneously couple to multiple diffraction channels. We show that the symmetry relation between absorptivity and emissivity can be broken in such multichannel emitters. The angular range in which the nonreciprocal effect is strong can also be significantly broadened. Such multichannel emitters can operate as one-way energy splitters. Our work significantly broadens the flexibility of thermal-radiation control in nonreciprocal thermal-emitter design.

DOI: 10.1103/PhysRevApplied.16.064001

I. INTRODUCTION

In recent years, there has been significant interest in designing thermal metamaterials to control conductive, convective, and radiative thermal transfer [1–4]. In particular, it has been noted for radiative thermal transfer that metamaterial structures allow us to reexamine some of the fundamental constraints [5].

For thermal radiation, one of the fundamental constraints is Kirchhoff's law. Kirchhoff's law of thermal radiation states that the absorptivity (α) and emissivity (ϵ) of an emitter satisfies $\alpha(\omega,\theta,\hat{p}) = \epsilon(\omega,-\theta,\hat{p}^*)$, as indicated in Figs. 1(a) and 1(b) [6–12]. Here, ω is the frequency; θ and $\hat{p}$ denote the angle of incidence and polarization, respectively, for incident light in the absorption case; and * denotes the complex conjugate. Kirchhoff's law provides the foundation for the design of almost all thermal emitters that we use in engineering. However, it is not a requirement of the second law of thermodynamics [5,13], and, in fact, the absorptivity and emissivity can be controlled separately if reciprocity is broken [14–18]. Nonreciprocal thermal emitters have significant promise in energy harvesting [19,20] and thermal management.

Recently, there have been several proposals of nonreciprocal thermal-emitter designs using magneto-optical materials or magnetic Weyl semimetals [11–13]. In these structures, incident light may be absorbed or reflected but is not diffracted, since the structures used are either subwavelength gratings or flat surfaces [15–17,21,22]. As we will illustrate in more detail here, for these structures, while the angular spectral emissivity and absorptivity are not equal [i.e., $\alpha(\omega,\theta) \neq \epsilon(\omega,\theta)$], they are nevertheless constrained by $\alpha(\omega,\theta) = \epsilon(\omega,-\theta)$, as illustrated in Fig. 1(c). (Throughout the paper, for simplicity, we consider only structures that preserve linear polarizations in the reflection process. Moreover, these structures exhibit violation of Kirchhoff's law only in p polarization. Thus, unless otherwise noted, all quantities that we discuss refer to p polarization.) This equality significantly restricts the ability to control the emissivity and absorptivity of these emitters separately. In addition, the angular range in which these structures exhibit a strong nonreciprocal effect is also restricted.

Here, we propose to use a metasurface with multiple diffraction channels [Fig. 1(d)] to remove the constraint of $\alpha(\omega,\theta) = \epsilon(\omega,-\theta)$ and create more flexibility in the design of nonreciprocal emitters. We prove that, in the absence of diffraction, $\alpha(\omega,\theta) = \epsilon(\omega,-\theta)$ always holds, regardless of detailed geometries of the structures. We provide a coupled-mode-theory framework for multichannel nonreciprocal emitters and derive the necessary conditions for the symmetry of the structure to achieve $\alpha(\omega,\theta) \neq \epsilon(\omega,-\theta)$. Based on theoretical discussions, we numerically demonstrate a multichannel nonreciprocal emitter

*shanhui@stanford.edu

†Current address: Department of Mechanical Engineering, University of Houston, Houston, Texas 77204, USA.

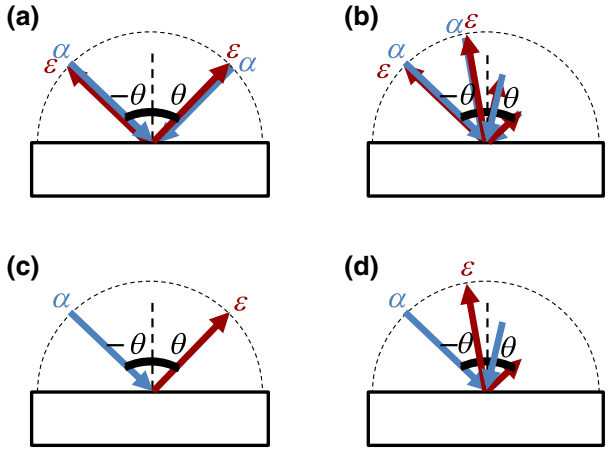

FIG. 1. Schematic of the angular distribution of emissivity and absorptivity in thermal emitters. (a) Reciprocal emitters with a reflection channel. (b) Reciprocal emitters with multiple diffraction channels. (c) Nonreciprocal emitters with a reflection channel. (d) Nonreciprocal emitters with multiple diffraction channels.

and showcase a one-way energy-splitting functionality as well as a broadened angular range of the nonreciprocal effect.

II. SCATTERING MATRIX AND ENERGY BALANCE IN THERMAL EMITTERS

We start by considering a general thermal emitter that is in thermal equilibrium with its surrounding ambient conditions, as shown in Fig. 2(a). We assume that the materials in the thermal emitter are linear and time invariant. We also assume that the bottom side of the emitter is a perfect mirror, so that thermal emission and absorption occur only to the top side. We refer to a plane-wave channel that couples to such a thermal emitter as a port. Within each port, there are input (s_+) and output waves (s_-) that are time reversals of each other. The emitter has m (≥ 1) ports in total, as illustrated in Fig. 2(a). We define an amplitude-reflection coefficient from port m to port m' as $r_{m'm}$. (The amplitude-reflection coefficient is defined as the ratio between the amplitudes of the reflected and the incident waves.) The power reflectivity can therefore be written as $R_{m'm} = |r_{m'm}|^2$. $r_{m'm}$ is the matrix element of scattering matrix $\mathbf{S}$. The absorptivity for light incident from port m can be written as

$$\alpha_m = 1 - \sum_{m'=1}^{M} R_{m'm}, \tag{1}$$

where M is the total number of ports. To determine the emissivity, we assume that each port is coupled to a blackbody at the same temperature as the emitter. Since the absorptivity of the blackbody is unity in the direction of port m, the emissivity of port m can also be related to the reflectivity as

$$\varepsilon_m = 1 - \sum_{m'=1}^{M} R_{mm'}. \tag{2}$$

Equations (1) and (2) are applicable for both reciprocal and nonreciprocal thermal emitters. For reciprocal emitters, since the scattering matrix is symmetric [23], one has $R_{m'm} = R_{mm'}$. Therefore, based on Eqs. (1) and (2), one obtains Kirchhoff's law

$$\alpha_m = \varepsilon_m. \tag{3}$$

In the case where reciprocity is broken, generally $R_{m'm} \neq R_{mm'}$ and therefore $\alpha_m \neq \varepsilon_m$.

The emissivity and absorptivity in Eqs. (1) and (2) are expressed in the wavevector space for each discretized plane-wave channel. To connect them with the same quantities expressed in angular coordinates, one can express the in-plane wavevector component that characterizes each port as

$$k_x = k_0 \sin\theta \cos\phi, \tag{4}$$

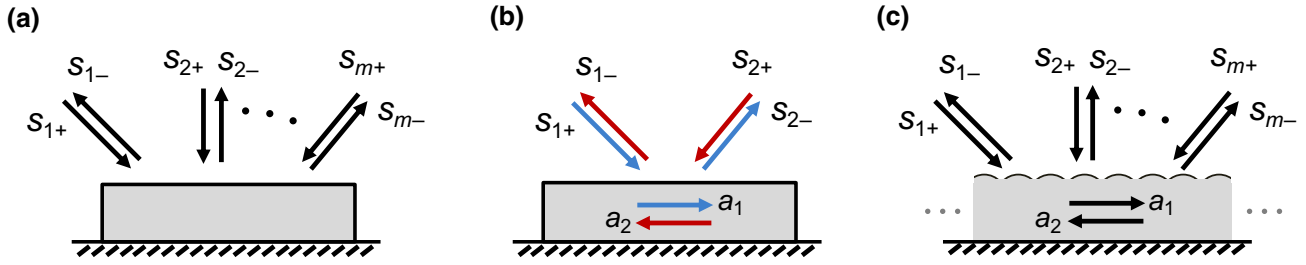

FIG. 2. (a) Schematic of a thermal emitter with multiple diffraction channels. (b) Thermal emitter with one reflection channel. a_1 and a_2 are two resonant modes of the emitter with opposite in-plane wavevectors. They couple to input and output waves of the same color. (c) Periodic metasurface thermal emitter with multiple diffraction channels. a_1 and a_2 are two modes with opposite in-plane wavevectors. Modes can couple to input and output waves from port 1 to m.

and

$$k_y = k_0 \sin\theta \sin\phi, \tag{5}$$

where $k_0 = \omega_0/c$, with c being the speed of light in vacuum, θ is the polar angle, and ϕ is the azimuthal angle. Therefore, we can define $\alpha(\omega, k_x, k_y) \equiv \alpha_m$, where (k_x, k_y) is the wavevector corresponding to the mth port. On the other hand, the wavevector and angular characteristics of absorptivity can be related using the Jacobian determinant of the transformation of Eqs. (4) and (5) as

$$\frac{1}{k_0^2}\alpha_m(\omega, k_x, k_y)dk_x dk_y = \alpha(\omega, \theta, \phi)\cos\theta \sin\theta \, d\theta d\phi. \tag{6}$$

A similar relationship can be derived for emissivity. Therefore, one can relate the absorptivity and emissivity for different ports to the angular dependency of the absorptivity and emissivity commonly used to described thermal emitters.

From Eqs. (1) and (2), we can obtain

$$\sum_m \alpha_m = \sum_m \varepsilon_m. \tag{7}$$

This is equivalent to

$$\int_0^{2\pi} d\phi \int_0^{\pi/2} \alpha(\omega, \theta, \phi)\cos\theta \sin\theta d\theta = \int_0^{2\pi} d\phi \int_0^{\pi/2} \varepsilon(\omega, \theta, \phi)\cos\theta \sin\theta d\theta. \tag{8}$$

Equations (7) and (8) show that the total absorption and emission of an emitter has to be the same, as required by energy conservation. These relationships are applicable for both reciprocal and nonreciprocal emitters.

We now consider a special case [Fig. 2(b)] where the structure does not have diffraction. Such a structure can be either a flat surface or a grating structure with subwavelength periodicity. For a plane-wave input from port 1, there is only one plane wave in the reflected wave in port 2. From Eqs. (1) and (2), one has

$$\alpha_1 = 1 - R_{21}, \tag{9}$$
$$\varepsilon_1 = 1 - R_{12}, \tag{10}$$
$$\alpha_2 = 1 - R_{12}, \tag{11}$$
$$\varepsilon_2 = 1 - R_{21}. \tag{12}$$

From Eqs. (9)–(12), we obtain

$$\alpha_1 = \varepsilon_2, \tag{13}$$

and

$$\varepsilon_1 = \alpha_2. \tag{14}$$

Due to the translational symmetry of the structure, the angle of incidence is equal to the angle of reflection. Therefore, from Eqs. (13) and (14), we have $\epsilon(\theta) = \alpha(-\theta)$. Equations (13) and (14) are consistent with the conclusions in Refs. [14,15].

III. COUPLED-MODE THEORY FOR NONRECIPROCAL METASURFACE EMITTERS

In the previous section, we see that, for the structure shown in Fig. 2(b), there are still strong constraints on its absorptivity and emissivity, even if the structure is nonreciprocal. Below, we will seek to design structures that are free from such constraints, by considering the multichannel thermal emitters shown in Fig. 2(c). These structures consist of gratings or metasurfaces, with a periodicity comparable to or larger than the wavelength of incident light. For such structures, an input plane wave can be reflected into multiple diffraction channels.

We use temporal coupled-mode theory to obtain the expression of reflection coefficients, absorptivity, and emissivity for such multichannel thermal emitters. Due to the periodicity, the modes in the metasurface are well characterized by the in-plane wavevector. We assume the modes are well separated in frequency, so that they can be analyzed separately. We denote the amplitude of excited mode a. With the excitation of the incoming wave, the dynamics of the mode amplitude can be described as [23–26]

$$\frac{da}{dt} = (i\omega_0 - \gamma^i - \gamma^r)a + \mathbf{k}^T\mathbf{s}_+, \tag{15}$$
$$\mathbf{s}_- = \mathbf{C}\mathbf{s}_+ + \mathbf{d}a. \tag{16}$$

We normalize the components such that $|a|^2$ represents the energy per unit area in the mode. ω_0 is the resonant angular frequency. γ^i and γ^r are the decay rates due to material loss and radiation loss, respectively. Here, the incoming wave has the same frequency as the mode. In general, their amplitudes are represented by

$$\mathbf{s}_+ = \begin{pmatrix} s_{1+} \\ s_{2+} \\ \vdots \\ s_{m+} \end{pmatrix}. \tag{17}$$

The incoming waves are coupled to the mode with the in-coupling rate given by

$$\mathbf{k} = \begin{pmatrix} k_1 \\ k_2 \\ \vdots \\ k_m \end{pmatrix}. \tag{18}$$

The excited resonance modes couple with the outgoing waves

$$\mathbf{s}_- = \begin{pmatrix} s_{1-} \\ s_{2-} \\ \vdots \\ s_{m-} \end{pmatrix}, \tag{19}$$

and the out-coupling rates are denoted as

$$\mathbf{d} = \begin{pmatrix} d_1 \\ d_2 \\ \vdots \\ d_m \end{pmatrix}. \tag{20}$$

Square matrix $\mathbf{C}$ in Eq. (16) describes the background-scattering process when the mode is absent. From Eq. (15), one obtains the mode amplitude as

$$a(\omega) = \frac{1}{i(\omega-\omega_0)+\gamma^i+\gamma^r}\mathbf{k}^T\mathbf{s}_+. \tag{21}$$

Using Eqs. (16) and (21), we have

$$\mathbf{s}_- = \mathbf{S}\mathbf{s}_+ = \left[\mathbf{C} + \mathbf{d}\frac{\mathbf{k}^T}{i(\omega-\omega_0)+\gamma^i+\gamma^r}\right]\mathbf{s}_+, \tag{22}$$

where $\mathbf{S}$ is the scattering matrix. We, therefore, can obtain the reflectivity from port m to port m' as

$$\begin{aligned} R_{m'm} &= \left|c_{m'm} + d_{m'}\frac{k_m}{i(\omega-\omega_0)+\gamma^i+\gamma^r}\right|^2. \\ &= |r_{m'm}|^2 \end{aligned} \tag{23}$$

If the loss rate of the material is neglected, the system is energy conserving, and one can obtain [23–26]

$$\mathbf{C}^\dagger\mathbf{C} = \mathbf{I}, \tag{24}$$

$$\mathbf{d}^\dagger\mathbf{d} = \mathbf{k}^\dagger\mathbf{k} = 2\gamma^r, \tag{25}$$

$$\mathbf{C}^{\mathrm{T}}\mathbf{d}^* = -\mathbf{k}, \tag{26}$$

$$\mathbf{C}\mathbf{k}^* = -\mathbf{d}. \tag{27}$$

Equations (24)–(27) hold for both reciprocal and nonreciprocal cases. In what follows, we assume that the material loss is small enough such that Eqs. (24)–(27) still hold. The effects of loss are then described only in terms of the presence of a nonzero intrinsic loss rate, γ^i, in Eqs. (21)–(23).

To describe the case where a plane wave is incident from port m, we set s_{m+} to be nonzero and all other components to be zero in Eq. (17). Based on Eq. (1), we have

$$\alpha_m = 1 - \frac{\mathbf{s}_-^\dagger\mathbf{s}_-}{\mathbf{s}_+^\dagger\mathbf{s}_+} = 1 - \frac{\mathbf{s}_+^\dagger\mathbf{S}^\dagger\mathbf{S}\mathbf{s}_+}{\mathbf{s}_+^\dagger\mathbf{s}_+} = \frac{2\gamma^i k_m^* k_m}{(\omega-\omega_0)^2+(\gamma^i+\gamma^r)^2}. \tag{28}$$

In deriving Eq. (28), we use

$$\mathbf{S}^\dagger\mathbf{S} = \mathbf{I} - \frac{2\gamma^i\mathbf{k}^*\mathbf{k}^{\mathrm{T}}}{(\omega-\omega_0)^2+(\gamma^i+\gamma^r)^2}. \tag{29}$$

Equation (29) is obtained using Eqs. (24)–(26).

Similarly, we can obtain the emissivity to port m. Comparing Eqs. (1) and (2), we notice that the only difference between the two equations is that the two indices of R are interchanged. Therefore, we can repeat the above derivation with $\mathbf{S}$ replaced by $\mathbf{S}^T$ in Eq. (28) to obtain

$$\varepsilon_m = 1 - \frac{\mathbf{s}_+^\dagger\mathbf{S}^*\mathbf{S}^T\mathbf{s}_+}{\mathbf{s}_+^\dagger\mathbf{s}_+} = \frac{2\gamma^i d_m^* d_m}{(\omega-\omega_0)^2+(\gamma^i+\gamma^r)^2}. \tag{30}$$

In deriving Eq. (30), we use

$$\mathbf{S}^*\mathbf{S}^T = \mathbf{I} - \frac{2\gamma^i\mathbf{d}^*\mathbf{d}^T}{(\omega-\omega_0)^2+(\gamma^i+\gamma^r)^2}. \tag{31}$$

Equation (31) is obtained using Eqs. (24), (25), and (27).

Equations (28) and (30) provide a general description of the radiative properties of a thermal radiator in the coupled-mode framework. In the Appendix, we also provide direct proof of Eqs. (28) and (30) using temporal coupled-mode theory combined with the fluctuation-dissipation theorem [27]. We note that the above analysis is also applicable to the case where transmission is present [28–30], since one can describe the transmission in terms of additional ports on the other side of the structure.

IV. SYMMETRY CONSIDERATION

In coupled-mode theory, the emissivity and absorptivity are controlled by the in-coupling rate $\mathbf{k}$ and out-coupling rates $\mathbf{d}$. For reciprocal emitters, we have $\mathbf{k} = \mathbf{d}$ [23], and therefore Eqs. (28) and (30) can directly give Kirchhoff's law for each port. For nonreciprocal emitters, the in- and out-coupling rates are no longer equal. They are, however, still constrained by various symmetries. For the design of nonreciprocal thermal radiators, it is therefore important to discuss these symmetries.

As an illustration of the symmetry constraints, we consider the structure shown in Fig. 3(a). The structure is

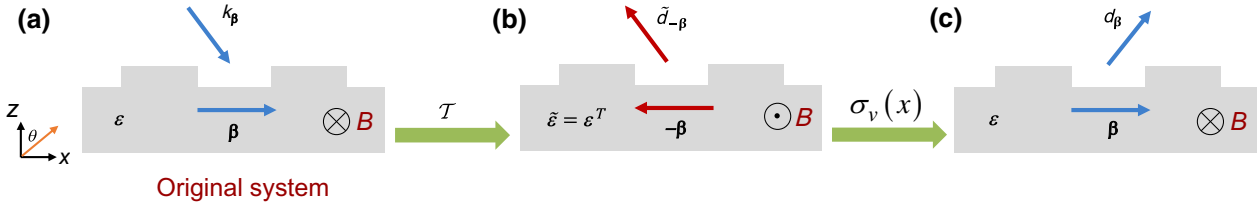

FIG. 3. Emitter with $\mathcal{T}\sigma_v(x)$ symmetry. (a) Original system. Emitter made of magneto-optical materials is colored gray and extended periodically in the x direction. (b) System obtained from (a) by a time-reversal operation, $\mathcal{T}$. (c) System obtained from (b) by the $\sigma_v(x)$ operation, which is a mirror operation with respect to the y-z plane.

periodic in the x direction. $\boldsymbol{\beta}$ is the in-plane wavevector that corresponds to the mode in the structure. We note that, when the incident light from a certain port couples to the mode at $\boldsymbol{\beta}$, the emission to the same port is due to the mode at $-\boldsymbol{\beta}$. We assume that the structure consists of a gyrotropic material with internal magnetization along the y direction. This internal magnetization can be due to an external magnetic field (B) along the y direction. The permittivity of such a gyrotropic material is then

$$\varepsilon(B) = \begin{bmatrix} \varepsilon_x & -i\varepsilon'(B) & 0 \\ i\varepsilon'(B) & \varepsilon_x & 0 \\ 0 & 0 & \varepsilon_z \end{bmatrix}, \tag{32}$$

where $-\varepsilon'(B) = \varepsilon'(-B)$, such that $\varepsilon^T(B) = \varepsilon(-B)$ satisfies the generalized Onsager reciprocal relationship [31–33].

Structures of the type in Fig. 3(a) have been previously studied in Refs. [15–18,22]. These studies noted that the angular distribution of emissivity and absorptivity exhibited the following relationship:

$$\varepsilon(\theta) = \alpha(-\theta). \tag{33}$$

In Eqs. (13) and (14) we provide a derivation of this constraint for an emitter, assuming that the emitter has no diffraction. Here, we provide an alternative derivation based on symmetry that is applicable to multichannel emitters with diffraction. We show that Eq. (33) holds for emitters with $\mathcal{T}\sigma_v(x)$ symmetry. Here, $\mathcal{T}$ is an "antisymmetry" operator that transforms $\epsilon(\mathbf{r})$ into $\epsilon^T(\mathbf{r})$, and $\sigma_v(x)$ denotes the mirror operation with respect to the y-z plane.

Figure 3(a) illustrates a structure with $\mathcal{T}\sigma_v(x)$ symmetry. Below, we discuss the constraint imposed by such a symmetry on the coupled-mode theory formalism of Eqs. (15) and (16). In our development above, the constraints on the coupling constants [Eqs. (24)–(27)] are derived assuming a lossless system first. Therefore, similarly, here, we derive the constraint on the coupling constants imposed by $\mathcal{T}\sigma_v(x)$ symmetry by first considering the lossless system.

For such a lossless system, the antisymmetry operator $\mathcal{T}$ is equivalent to the time-reversal operator. Consider the process, as shown in Fig. 3(a), where an incident plane wave excites a resonant mode in the structure with wavevector $\boldsymbol{\beta}$, through an in-coupling constant k_β. By applying the time-reversal operation to the structure and the process in Fig. 3(a), we arrive at Fig. 3(b). Here, the structure becomes the complementary structure of Fig. 3(a), with the magnetization direction flipped from that of Fig. 3(a), and the process becomes a resonant mode with wavevector $-\boldsymbol{\beta}$ exciting an outgoing plane wave with an out-coupling constant $\tilde{d}_{-\beta}$. Thus, we expect that

$$k_\beta = \tilde{d}_{-\beta}, \tag{34}$$

and a similar derivation can be used to show that

$$d_\beta = \tilde{k}_{-\beta}. \tag{35}$$

From the system shown in Fig. 3(b), we further apply a mirror-reflection operation of $\sigma_v(x)$ to arrive at the system shown in Fig. 3(c). In Fig. 3(c), the structure including the direction of magnetization is the same as that in Fig. 3(a), and the process corresponds to a resonant mode at $\boldsymbol{\beta}$ radiating into an outgoing wave with an out-coupling constant, d_β. Therefore, we have

$$\tilde{d}_{-\beta} = d_\beta, \tag{36}$$

and

$$\tilde{k}_{-\beta} = k_\beta. \tag{37}$$

Also from Eq. (36), as well as the connection between the decay rate γ and the out-coupling rate d, we have

$$\tilde{\gamma}^i_{-\beta} = \gamma^i_\beta. \tag{38}$$

Combining Eqs. (34) and (36), we obtain

$$k_\beta = d_\beta. \tag{39}$$

Since k_β and d_β belong to the ports that are symmetric with respect to the y-z mirror plane, based on Eqs. (28), (30),

and (39) implies

$$\varepsilon_m = \alpha_n, \tag{40}$$

where m and n are the labels for ports that are symmetric with respect to the y-z mirror plane. Equation (40) is equivalent to Eq. (33). Therefore, the emissivity and absorptivity of structures with $\mathcal{T}\sigma_v(x)$ symmetry are constrained by Eq. (33).

Combining the discussion here with the discussion on the scattering matrix in the previous section, we see that, to remove the constraints of Eq. (33), one must consider a multichannel emitter without $\mathcal{T}\sigma_v(x)$ symmetry.

V. NUMERICAL DEMONSTRATION OF MULTIPORT NONRECIPROCAL THERMAL EMITTERS

As a demonstration of the conclusions obtained above, we numerically study two cases shown in Figs. 4(a) and 4(c). We consider the radiative property of transverse magnetic waves (magnetic field in the y direction) at a wavelength of $\lambda = 15\ \mu$m. Both emitter designs are metal-dielectric-metal structures. The top layer contains two types of metal strips arranged periodically with a period of $\Lambda = 20\ \mu$m, and their widths are $b_1 = 3.08\ \mu$m and $b_2 = 4.93\ \mu$m. Here, $\Lambda > \lambda$ and therefore both emitters have multiple diffraction channels. The thicknesses of the strips and the dielectric layer are 0.68 and 1.1 μm, respectively. The substrate is made of the same material as the strips and is assumed to be infinitely thick. The dielectric function of the dielectric layer is $\varepsilon_d = 10.25 + 0.052i$, close to that of SiC and Si at the wavelength of 15 μm. The metal has the same property as that shown in Eq. (32), with $\varepsilon_x = \varepsilon_z = -76.5 + 0.014i$ and $\varepsilon' = 26.62$, which is close to the properties of Weyl semimetals at a wavelength of 15 μm [17,18,34–36].

In the structure shown in Fig. 4(a), the centers of the strips are separated by half the period. Therefore, the structure possesses $\mathcal{T}\sigma_v(x)$ symmetry. As shown in Fig. 4(b), the angular distributions of emissivity and absorptivity are symmetric with respect to $\theta = 0°$, and therefore, satisfies Eq. (33). In Fig. 4(c), we shift one of the strips slightly along the x direction to break $\mathcal{T}\sigma_v(x)$ symmetry. As shown in Fig. 4(d), the angular distributions of emissivity and absorptivity are no longer symmetric with respect to $\theta = 0°$, and therefore the constraint of Eq. (33) is broken. We therefore provide a numerical illustration of the symmetry constraint, as we discuss above for multichannel nonreciprocal thermal emitters.

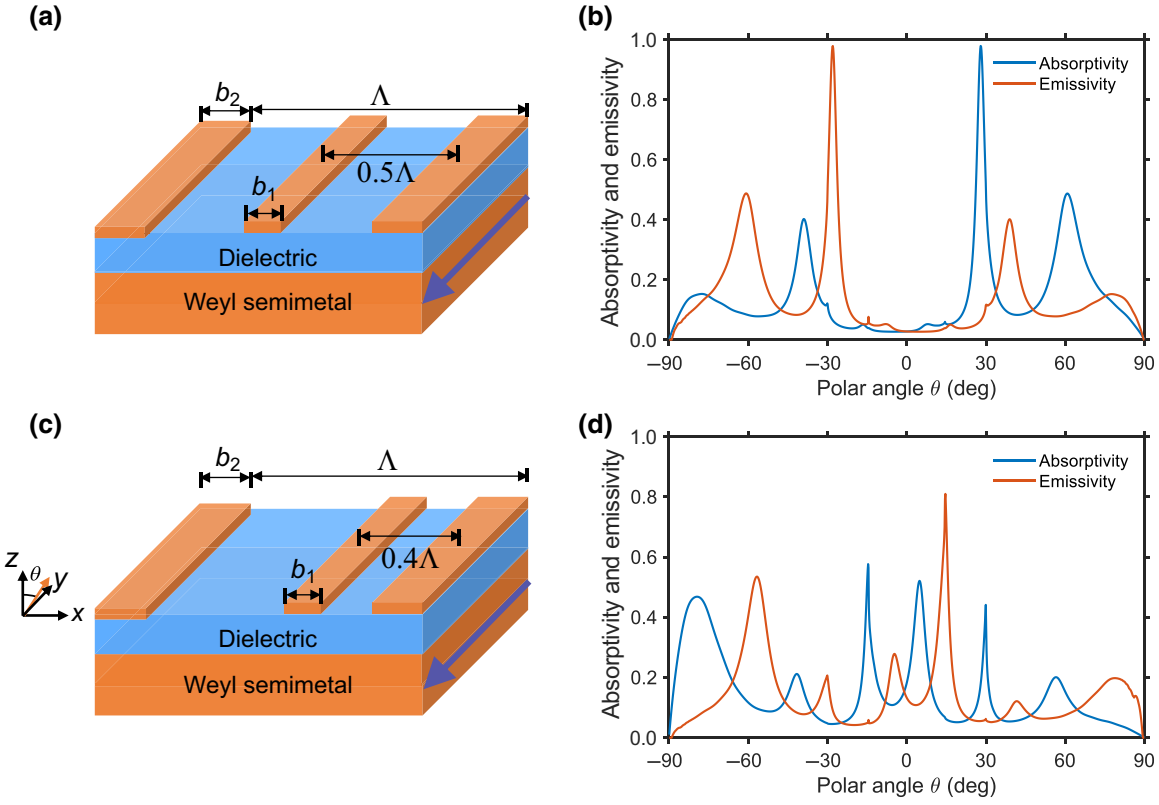

FIG. 4. (a),(c) Schematic of nonreciprocal multiport emitters. (a) With $\mathcal{T}\sigma_v(x)$ symmetry. (c) Without $\mathcal{T}\sigma_v(x)$ symmetry. (b),(d) Angular distribution of emissivity and absorptivity for structures in (a),(c) respectively. Arrow indicates the direction of Weyl node separation, which breaks the reciprocity in the same way as an external B field.

Compared with previously reported nonreciprocal emitters [15–18,22], at the operating wavelength, the multichannel emitters provide a much broader angular range where the nonreciprocal effect is prominent. Moreover, the structures in Figs. 4(a) and 4(c) can operate as nonreciprocal energy splitters. For example, for the case in Fig. 4(a), incident energy at $\lambda = 15\ \mu$m from $\theta = 28^\circ$ will be nearly completely absorbed, whereas the emission at the same wavelength primarily goes to the directions of $\theta = -60.9^\circ$, -28°, and 38.9°, splitting of the incident energy. This functionality may provide additional flexibilities in the control of the flow of thermal radiation.

VI. CONCLUSION

We show that the angular distribution of emissivity and absorptivity is mirror symmetric with respect to the normal direction for nondiffracting thermal emitters and metasurfaces with $\mathcal{T}\sigma_v(x)$ symmetry. To break this symmetry, one needs to use multiport nonreciprocal metasurface emitters without $\mathcal{T}\sigma_v(x)$ symmetry. Our theory can provide guidance for designing nonreciprocal thermal emitters and optical devices with much more angular degree of freedom.

ACKNOWLEDGMENTS

This work is supported by the Defense Advanced Research Projects Agency under Grant No. HR0011182 0046 (theoretical calculations), and by the U.S. Department of Energy Photonics at the Thermodynamic Limits Energy Frontier Research Center under Grant No. DE-SC0019140 (numerical simulations).

APPENDIX: TEMPORAL COUPLED-MODE THEORY AND FLUCTUATION-DISSIPATION THEOREM

Thermal radiation from a resonator structure can be described using the coupled-mode equation [27]:

$$\frac{da}{dt} = (i\omega_0 - \gamma^i - \gamma^r)a + \mathbf{k}^T\mathbf{s}_+ + \sqrt{2\gamma^i}n, \tag{A1}$$

where n is the noise source with its correlation described by the fluctuation-dissipation theorem:

$$\langle n(\omega)n^*(\omega')\rangle = \frac{1}{2\pi}\Theta(\omega, T)\delta(\omega - \omega'). \tag{A2}$$

In Eq. (A2), $\Theta(\omega, T) = \hbar\omega/[exp(\hbar\omega/k_BT) - 1]$ is the mean thermal energy in a mode at frequency ω. We consider the thermal emitter shown in Fig. 2(a) of the main text. To compute the emission, we assume that the ambient temperature, T_{amb}, is 0 K; therefore, there is no incoming thermal radiation, $s_+ = 0$.

The ensemble-averaged outgoing power of port m is described as

$$\begin{aligned}
\langle P_m^e(t)\rangle &= \langle s_{m-}(t)s_{m-}^*(t)\rangle = d_m^*d_m\langle a(t)a^*(t)\rangle, \\
&= d_m^*d_m\int_0^{+\infty}d\omega'\int_0^{+\infty}\langle a(\omega)a^*(\omega')\rangle exp[i(\omega' - \omega)t]d\omega, \\
&= d_m^*d_m\int_0^{+\infty}d\omega'\int_0^{+\infty}\left[\frac{\sqrt{2\gamma^i}}{i(\omega - \omega_0) + \gamma^i + \gamma^r}\frac{\sqrt{2\gamma^i}}{-i(\omega' - \omega_0) + \gamma^i + \gamma^r}\langle n(\omega)n^*(\omega')\rangle\right]exp[i(\omega' - \omega)t]d\omega, \\
&= \int_0^{+\infty}\frac{1}{2\pi}\Theta(\omega, T)\frac{2\gamma^i d_m^*d_m}{(\omega - \omega_0)^2 + (\gamma^i + \gamma^r)^2}d\omega.
\end{aligned} \tag{A3}$$

The emitted power spectrum in port m is therefore

$$P_m^e(\omega) = \frac{2\gamma^i d_m^*d_m}{(\omega - \omega_0)^2 + (\gamma^i + \gamma^r)^2}\frac{1}{2\pi}\Theta(\omega, T). \tag{A4}$$

The spectral power density emitted from a blackbody at ω is [27]

$$P_{\text{BB}}(\omega) = \frac{1}{2\pi}\Theta(\omega, T). \tag{A5}$$

We therefore can obtain the emissivity for port m as

$$\varepsilon_m = \frac{P_m^e(\omega)}{P_{\text{BB}}(\omega)} = \frac{2\gamma^i d_m^*d_m}{(\omega - \omega_0)^2 + (\gamma^i + \gamma^r)^2}. \tag{A6}$$

We therefore prove Eq. (30).

For the absorption process, we again consider the thermal emitter shown in Fig. 2(a) of the main text. We assume an ambient temperature of $T_{\text{amb}} > 0$ K and assume that the thermal emitter is at 0 K. Therefore, the contribution of the intrinsic noise source is zero. We consider the case when

port m has input from the ambient conditions, which can be treated as a blackbody,

$$\frac{da}{dt} = (i\omega_0 - \gamma^i - \gamma^r)a + \mathbf{k}^T\mathbf{s}_+, \tag{A7}$$

where $s_{m+} = n_{\text{amb}}$ and $\langle n_{\text{amb}}(\omega) {n_{\text{amb}}}^*(\omega')\rangle = \frac{1}{2\pi}\Theta(\omega, T)\,\delta(\omega - \omega')$, and the rest component of $\mathbf{s}_+$ is zero. Therefore,

$$a(\omega) = \frac{k_m n_{\text{amb}}(\omega)}{i(\omega - \omega_0) + \gamma^i + \gamma^r}. \tag{A8}$$

The dissipated power can be obtained directly by

$$\begin{aligned}\left\langle P_m^a(t)\right\rangle &= 2\gamma^i\left\langle a(t)a^*(t)\right\rangle,\\ &= 2\gamma^i\int_0^{+\infty}d\omega'\int_0^{+\infty}\left\langle a(\omega)a^*(\omega')\right\rangle\\ &\quad\times\exp[i(\omega' - \omega)t]d\omega,\\ &= \int_0^{+\infty}\frac{1}{2\pi}\Theta(\omega, T_{\text{amb}})\frac{2\gamma^i k_m^* k_m}{(\omega - \omega_0)^2 + (\gamma^i + \gamma^r)^2}d\omega.\end{aligned} \tag{A9}$$

Therefore, the absorbed power spectrum in port m can be obtained as

$$P_m^a(\omega) = \frac{1}{2\pi}\Theta(\omega, T_{\text{amb}})\frac{2\gamma^i k_m^* k_m}{(\omega - \omega_0)^2 + (\gamma^i + \gamma^r)^2}. \tag{A10}$$

We therefore can obtain the absorptivity for port m as

$$\alpha_m = \frac{P_m^a(\omega)}{P_{\text{BB}}(\omega)} = \frac{2\gamma^i k_m^* k_m}{(\omega - \omega_0)^2 + (\gamma^i + \gamma^r)^2}. \tag{A11}$$

We thus prove Eq. (28).

[1] Y. Li, W. Li, T. Han, X. Zheng, J. Li, B. Li, S. Fan, and C.-W. Qiu, Transforming heat transfer with thermal metamaterials and devices, Nat. Rev. Mater. **6**, 488 (2021).

[2] S. R. Sklan and B. Li, Thermal metamaterials: Functions and prospects, Natl. Sci. Rev. **5**, 138 (2018).

[3] J.-P. Huang, *Theoretical Thermotics: Transformation Thermotics and Extended Theories for Thermal Metamaterials* (Springer, Singapore, 2020).

[4] D. G. Baranov, Y. Xiao, I. A. Nechepurenko, A. Krasnok, A. Alù, and M. A. Kats, Nanophotonic engineering of far-field thermal emitters, Nat. Mater. **18**, 920 (2019).

[5] S. Fan, Thermal photonics and energy applications, Joule **1**, 264 (2017).

[6] G. Kirchhoff, Ueber das Verhältniss zwischen dem Emissionsvermögen und dem Absorptionsvermögen der Körper für Wärme und Licht, Ann. Phys. (Berl.) **185**, 275 (1860).

[7] M. Planck, *The Theory of Heat Radiation* (Forgotten Books, London, 2013).

[8] J. R. Howell, M. P. Menguc, K. Daun, and R. Siegel, *Thermal Radiation Heat Transfer*, 7th ed. (CRC Press, Florida, 2021).

[9] T. L. Bergman, A. S. Lavine, F. P. Incropera, and D. P. DeWitt, *Fundamentals of Heat and Mass Transfer* (Wiley, Hoboken, NJ, 2017).

[10] G. Chen, *Nanoscale Energy Transport and Conversion* (Oxford University Press, Inc, New York, 2005).

[11] M. F. Modest, *Radiative Heat Transfer*, 3nd ed. (Academic Press, Oxford, 2013).

[12] Z. M. Zhang, *Nano/Microscale Heat Transfer* (McGraw-Hill, New York, 2007).

[13] L. D. Landau, E. M. Lifshitz, and L. P. Pitaevskii, *Electrodynamics of Continuous Media*, 2nd ed. (Pergamon Press, Oxford, 1984).

[14] D. A. B. Miller, L. Zhu, and S. Fan, Universal modal radiation laws for all thermal emitters, Proc. Natl. Acad. Sci. U.S.A. **114**, 4336 (2017).

[15] L. Zhu and S. Fan, Near-complete violation of detailed balance in thermal radiation, Phys. Rev. B **90**, 220301 (2014).

[16] B. Zhao, Y. Shi, J. Wang, Z. Zhao, N. Zhao, and S. Fan, Near-complete violation of Kirchhoff's law of thermal radiation with a 0.3 T magnetic field, Opt. Lett. **44**, 4203 (2019).

[17] B. Zhao, C. Guo, C. A. C. Garcia, P. Narang, and S. Fan, Axion-field-enabled nonreciprocal thermal radiation in Weyl semimetals, Nano Lett. **20**, 1923 (2020).

[18] Y. Tsurimaki, X. Qian, S. Pajovic, F. Han, M. Li, and G. Chen, Large nonreciprocal absorption and emission of radiation in type-I Weyl semimetals with time reversal symmetry breaking, Phys. Rev. B **101**, 165426 (2020).

[19] P. T. Landsberg and G. Tonge, Thermodynamic energy conversion efficiencies, J. Appl. Phys. **51**, R1 (1980).

[20] M. A. Green, Time-asymmetric photovoltaics, Nano Lett. **12**, 5985 (2012).

[21] Z. M. Zhang, X. Wu, and C. Fu, Validity of kirchhoff's law for semitransparent films made of anisotropic materials, J. Quant. Spectrosc. Radiat. Transfer **245**, 106904 (2020).

[22] X. Wu, R. Liu, H. Yu, and B. Wu, Strong nonreciprocal radiation in magnetophotonic crystals, J. Quant. Spectrosc. Radiat. Transfer **272**, 107794 (2021).

[23] Z. Zhao, C. Guo, and S. Fan, Connection of temporal coupled-mode-theory formalisms for a resonant optical system and its time-reversal conjugate, Phys. Rev. A **99**, 033839 (2019).

[24] S. Fan, W. Suh, and J. D. Joannopoulos, Temporal coupled-mode theory for the fano resonance in optical resonators, J. Opt. Soc. Am. A **20**, 569 (2003).

[25] W. Suh, Z. Wang, and S. Fan, Temporal coupled-mode theory and the presence of non-orthogonal modes in lossless multimode cavities, IEEE J. Quantum Electron. **40**, 1511 (2004).

[26] K. X. Wang, Time-reversal symmetry in temporal coupled-mode theory and nonreciprocal device applications, Opt. Lett. **43**, 5623 (2018).

[27] L. Zhu, S. Sandhu, C. Otey, S. Fan, M. B. Sinclair, and T. S. Luk, Temporal coupled mode theory for thermal emission from a single thermal emitter supporting either a single mode or an orthogonal set of modes, Appl. Phys. Lett. **102**, 103104 (2013).

[28] Y. Park, V. S. Asadchy, B. Zhao, C. Guo, J. Wang, and S. Fan, Violating Kirchhoff's law of thermal radiation in semitransparent structures, ACS Photonics **8**, 2417 (2021).

[29] Z. Yu, Z. Wang, and S. Fan, One-way total reflection with one-dimensional magneto-optical photonic crystals, Appl. Phys. Lett. **90**, 121133 (2007).

[30] V. S. Asadchy, C. Guo, B. Zhao, and S. Fan, Subwavelength passive optical isolators using photonic structures based on Weyl semimetals, Adv. Opt. Mater. **8**, 2000100 (2020).

[31] L. Onsager, Reciprocal relations in irreversible processes. I, Phys. Rev. **37**, 405 (1931).

[32] L. Onsager, Reciprocal relations in irreversible processes. II, Phys. Rev. **38**, 2265 (1931).

[33] H. B. G. Casimir, On Onsager's principle of microscopic reversibility, Rev. Mod. Phys. **17**, 343 (1945).

[34] O. V. Kotov and Y. E. Lozovik, Giant tunable nonreciprocity of light in Weyl semimetals, Phys. Rev. B **98**, 195446 (2018).

[35] J. Hofmann and S. Das Sarma, Surface plasmon polaritons in topological Weyl semimetals, Phys. Rev. B **93**, 241402 (2016).

[36] O. V. Kotov and Y. E. Lozovik, Dielectric response and novel electromagnetic modes in three-dimensional dirac semimetal films, Phys. Rev. B **93**, 235417 (2016).